Identification and characterization of compounds that improve plant photosynthesis and growth under light stress conditions

Check for updates

Yuchen Qu[1], Kazuma Sakoda[1,2], Yu Wakabayashi[1], Masatoshi Nakajima[3], Tadao Asami[3], Ichiro Terashima[1,4] & Wataru Yamori[1] ✉

To meet the escalating food and fuel demands of a growing global population and industry, food production requires a 50% increase by 2050. However, various environmental stresses, such as excessive light, significantly inhibit plant growth and lead to substantial reductions in crop yields. A major contributing factor to such declines is the reduction in photosynthetic capacity. In this study, a chemical-screening system based on standard 96-well plate and tobacco leaf tissue was developed. With this system, several anthraquinone derivatives that could alleviate high light stress from plants were identified. Application of these chemicals induced greater photosynthetic capacities and better plant growth during and after exposure to light stress for 20-96 hours in tobacco, lettuce, tomato and Arabidopsis. Mechanistic investigations unveiled that these chemicals exhibited electron-accepting abilities at PSI in vitro and improve PSI efficiency in vivo, indicating that the photoprotective effect could be a result of PSI acceptor side oxidation induced by these chemicals. Meanwhile, no adverse effects on plant growth were observed in chemical treated plants under non-stressful cultivation conditions. This study implies that anthraquinone derivatives can confer high light stress tolerance in plants, resulting in improved plant photosynthesis and growth in light stress environments.

The world's population may reach 10 billion by 2050, but around 10% currently suffer from food shortages (UN, 2019; FAOSTAT, 2019). Furthermore, natural disasters, such as droughts, floods, and extreme temperatures caused by climate changes, are now becoming a threat to agricultural production[1], and 91% of farmland is impacted by some type of stress, which will eventually result in decreases in grain yields[2]. Decreases in plant productivity are primarily caused by reduced photosynthetic ability because of stress damage[3,4]. It is well known that plants are sensitive to changes in their environment, and fluctuations in natural conditions may result in stress and hinder the growth and yield of plants by up to 50%[5–9]. Such conditions include drought (water stress), excessive watering (waterlogging), extreme temperatures (cold, frost, and heat), salinity, and mineral toxicity. Nevertheless, increased anniversary light intensity (light stress) induced by climate changes plays an unneglectable role[10]. Therefore, improving photosynthesis under stressful conditions is especially important to ensure agricultural productivity and food safety in the near future[11].

As an energy source, light is critical for photosynthesis. Plants absorb light at photosystem II (PSII) and I (PSI), giving impetus to the flow of electrons through the electron transport chain, and they eventually turn light energy into ATP and NADPH. ATP and NADPH are consumed in the Calvin cycle, where CO_2 is reduced and generally assimilated in the form of organic compounds. However, plants frequently get exposed to high light intensities and are photodamaged, resulting in them being unable to utilize all the captured light energy for photosynthesis[12–14]. When electron consumption in the CO_2 assimilation process is no longer sufficient to cope with electron generation, excessive energy starts to accumulate in chloroplasts, resulting in light stress[12–14]. Usually, this results in the generation of reactive oxygen species (ROS), which are induced by direct reductions of O_2[12,15], or PSI acceptor side over-reduction, leading to a decrease in PSI oxidization

[1]Graduate School of Agricultural and Life Sciences, The University of Tokyo, Nishitokyo, Tokyo, 188-0002, Japan. [2]Space Environment and Energy Laboratories, NTT Corporation, Musashino, Tokyo, Japan. [3]Graduate School of Agricultural and Life Sciences, The University of Tokyo, Bunkyo-ku, Tokyo, 113-8657, Japan. [4]Institute of Molecular Biology, National Chung Hsing University, South Dist, Taichung, 40227, Taiwan. ✉e-mail: yamori@g.ecc.u-tokyo.ac.jp

capacity due to P700 rapid charge recombination[16]. In fact, PSII damage from light stress is often observed in field conditions[17], and it is generally considered that PSII is a primary target for photoinhibition as a result of ROS accumulation[18]. Studies have shown that PSI damage caused by fluctuating light during the day or over-reduction of the electron transport chain in high-light conditions is relatively common and can result in decreased photosynthesis, growth, and yields[4,19–22]. One major area of research for improving plant tolerance against light stress is through genetic modifications. There has been much research into the biosynthesis of carotenoids[23], flavonols[24], chloroplastic prenyl lipids[25], and melatonin[26] combined with modifications to the xanthophyll cycle[27]. Recent studies have shown that the introduction of maize GOLDEN2-LIKE genes into rice reduced photoinhibition and improved vegetative biomass and grain yields by 30–40% in strong light conditions[22], and introducing flavodiiron proteins of Physcomitrium patens into rice or Arabidopsis reduced photodamage during PSI in high light and fluctuating light conditions[28,29].

However, there are increasing concerns about the safety of planting and consuming genetically modified plants[30]. An alternative strategy for improving plant tolerance to light stress could be through chemical biology. Chemical biology is a discipline of biology that addresses biological phenomena by using small bioactive chemicals together with conventional biological techniques[31]. In the past two decades, such techniques have been widely explored with animal materials, from the cellular level to high-throughput screening methods for drug discoveries[32,33]. Recently, these techniques have also been used in plant research. Some chemical compounds have been found to be capable of inducing stomatal closure through ABA-dependent or ABA-independent signaling pathways[34,35], while other chemical compounds show commercial potential as candidate compounds for increasing the shelf life of cut flowers in the floral industry[36]. It has also been found that some chemicals can be utilized in the modification of essential proteins in the regulation of cell division and polarity, which improves stomatal development[37,38] and increases seedling biomass in Arabidopsis[39]. Furthermore, treatment with acetate triggers a dynamic metabolic flux conversion from glycolysis into acetate synthesis, which stimulates the jasmonate signaling pathway. This confers drought tolerance and improves the survival of Arabidopsis, maize, wheat, rice, and rape in extreme drought conditions[40]. However, despite these many breakthroughs, it seems that chemical compounds that regulate plant tolerance against light stress have barely been studied.

In this study, we constructed a chemical screening system to search for chemicals that could improve plant photosynthesis and growth under high-light conditions. Tobacco leaf disks were used as the major plant material. Screening through chemical libraries was performed based on photosynthetic imaging techniques, and several anthraquinone derivatives that could relieve high light stress from plants, not only in tobacco but also in other plant materials, including Arabidopsis, and lettuces, were identified. Further analyses showed that the photoprotective effect of anthraquinone derivatives is closely related to chemical-induced PSI oxidation. Meanwhile, no negative effects on plant growth were observed in chemical-treated plants under non-stressful conditions, implying that such chemicals have the potential to be used in the development of agricultural chemicals for broader applications.

Results
Screening a library of 12,000 chemicals
To identify compounds that affect plant tolerance under light stress conditions, we first screened 12,000 chemical compounds acquired from Maybridge Chemical Company Limited using the tobacco leaf disk system. Tobacco leaves have extremely large surface areas with uniformly featured photosynthetic activities, which can enable measuring the effect of the chemicals on a large scale. The entire screening process was divided into first and second screening sections. The first screening was performed with one replication for each chemical in order to achieve high throughput, and any chemical with a suspiciously positive effect would be further tested in the

second screening. For the second screening, each chemical was tested with three or more replications.

After two rounds of screening, 33 candidates that induced higher Fv/Fm or Y(II) at the initial or stable state of photosynthetic induction (actinic light is 200 μmol m^{-2} s^{-1} followed by 700 μmol m^{-2} s^{-1}) in leaf disks after high light stress treatment were identified out of the 12,000 chemicals. Among these candidates, nitrogen dioxide (-NO$_2$) residue was found in 27 chemicals, and cyanide (-C≡N) residue in six chemicals, making them dangerous or environmentally toxic[41,42]. Two anthraquinone derivatives (A4N, A18Ch) were considered to be generally safe and were selected for further study since they showed high potential in practical applications (Fig. 1C). In further analyses, we also used 10 structural analogs (A14N, A48N, A1N4C, A1N, A1458N, A1Ch, A14Ch, A14Ch23C, A1Ch2C, A4Ch1C) closely related to A4N and A18Ch (Fig. 1C).

Chlorophyll fluorescence of leaf disks before and after light stress treatment
The leaf disks were treated with 12 chemicals, and chlorophyll fluorescence was measured before and after high light stress at 700 μmol photons m^{-2} s^{-1} (Fig. 2). A18Ch, A1Ch, and A14Ch significantly decreased Fv/Fm even without light stress compared with the control group (Fig. S1A). A similar effect was observed in the DCMU and MV treatment groups (Fig. S1A). After light stress treatment, the A18Ch, A1Ch, and A14Ch treatment groups, together with the DCMU treatment group showed significantly lower Fv/Fm compared with the control group (Fig. S1B). The MV treatment group showed completely undetectable Fv/Fm (Fig. S1B). Other chemical treatment groups showed no significant differences in Fv/Fm compared with the control group before and after light stress (Fig. S1A, S1B).

The Y(II) of different groups before and after light stress treatment was also determined. The Y(II) of leaf disks adapted to dark environments often reaches its plateau value after an initial induction period from only several seconds to minutes after being exposed to a certain light intensity, which is called photosynthetic induction. In this study, photosynthetic induction of leaf disks was taken as a parameter to evaluate the effect of chemicals effect before and after light stress treatment. Y(II) at the initial state of photosynthetic induction (the first 30 seconds) and the steady state of photosynthesis (by the end of 310 s) were analyzed (Fig. 2A). At the initial state of photosynthetic induction, A1N, A1Ch2C, and A4Ch1C treatment groups showed significantly higher Y(II) than the control group, while the Y(II) of the DCMU treatment group was significantly lower than the control group (Fig. 2B). The A1N, A1Ch, and A14Ch treatment groups showed slightly higher Y(NPQ) compared with the control group, and the Y(NPQ) of the DCMU treatment group was lower than the control group (Fig. S1C). The A1N, A1Ch, A1Ch2C, and A4Ch1C treatment groups showed slightly higher qP and the DCMU treatment groups showed lower qP compared with the control group Fig. S1E). At the steady state of photosynthesis, the Y(II) of most chemical treatment groups showed no significant difference with the control group except for the A1Ch treatment group, which had significantly lower Y(II) than the control group (Fig. 2C). The Y(II) of the DCMU and MV treatment groups were also significantly lower than that of the control group due to PSII inhibition and cell damage (Fig. 2C). No significant difference in Y(NPQ) was observed except for the DCMU and MV treatment groups, which were significantly higher than the control group (Fig. S1D). Also, no significant difference in qP was observed except for the DCMU treatment group, which was significantly lower than the control group (Fig. S1F).

After light stress treatment for 12 h, photosynthetic induction of the control group appeared to be slower than most of the chemical treatment groups, while photosynthesis in the DCMU and MV treatment groups was almost undetectable (Fig. 2D). At the initial state of photosynthetic induction, A4N, A48N, A1N4C, A1N, A18Ch, A1Ch, A14Ch, A14Ch32C, A1Ch2C, and A4Ch1C treatment groups showed significantly higher Y(II) compared with the control group (Fig. 2E), and at the steady state of photosynthesis, A4N, A14N, A48N, A1N4C, A1N, A1458N, A14Ch23C, and A4Ch1C treatment groups showed significantly higher Y(II) compared with
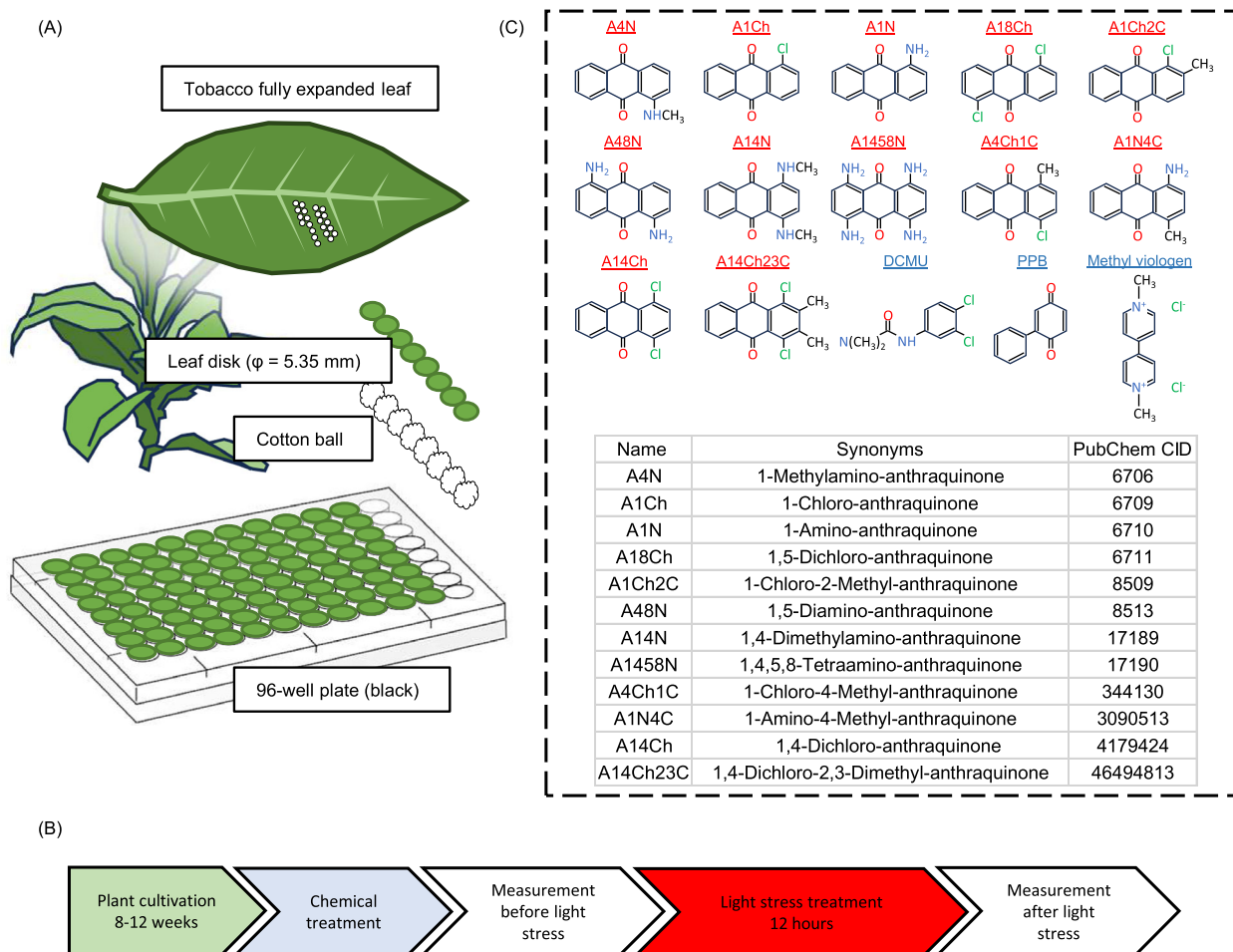
Fig. 1 | Constructing a screening system using tobacco leaf disks. A Leaf disks and 96-well plates were used as chemical screening tools in this study. **B** The process for performing the leaf disk chemical screening experiment. **C** Structural information of candidate chemicals that showed protective effects against light stress, together with three inhibitors/electron acceptors, which served as positive/negative controls.

the control group (Fig. 2F). Notably, the PPB treatment group showed significantly higher Y(II) at both the initial and steady state of photosynthesis, indicating a minor protective effect against light stress (Fig. 2E, F). In general, A4N, A48N, A1N4C, A1N, A14Ch23C, and A4Ch1C treatment groups showed significantly higher Y(II) compared with the control group throughout photosynthetic induction. The A18Ch, A1Ch, A14Ch, and A1Ch2C treatment groups showed significantly higher Y(II) at the initial state but not at the steady state of photosynthesis. The A14N and A1458N treatment groups showed significantly higher Y(II) at the steady state of photosynthesis, but no significant difference in these two groups was observed at the initial state of photosynthetic induction. At the initial state of photosynthetic induction after light stress treatment, A4N, A1N, A18Ch, A1Ch, A14Ch, A1Ch2C, and A4Ch1C treatment groups showed significantly lower Y(NPQ) compared with the control group, while the Y(NPQ) of the MV treatment group was not detectable (Fig. S1G). The A4N, A48N, A1N4C, A1N, A18Ch, A1Ch, A14Ch23C, A1Ch2C, and A4Ch1C treatment groups showed significantly higher qP compared with the control group, whereas the qP of the A4N, A1N, A18Ch, A1Ch, A1Ch2C, and A4Ch1C treatment groups was more than eight times higher than the control group (Fig. S1I). During the steady state of photosynthesis after light stress treatment, A4N, A48N, A1N, A18Ch, A14Ch, A14Ch23C, A1Ch2C, and A4Ch1C treatment groups showed significantly lower Y(NPQ) compared with the control group, while the Y(NPQ) of the MV treatment group was not detectable (Fig. S1H). The A1Ch and A14Ch treatment groups showed significantly lower qP compared with the control group, while the qP of the MV treatment group was not detectable (Fig. S1J).

In order to further confirm the relationship between chemical treatment and the improvement of photosynthesis after light stress treatment, we studied the concentration-dependency of the protective effect of A1N and A4N because these two chemicals showed significantly higher Y(II) at both the initial and steady state of photosynthesis after light stress treatment (Fig. 2E, F), and they are also similar in structure (Fig. 1C). We also used Anthraquinone (9,10-anthraquinone, ANTQ) for treatments to see if similar effects could be observed with the skeletal structure alone. The chemicals were applied at different concentrations. After exposure to light stress at 700 μmol photons $m^{-2} s^{-1}$, the Y(II) of leaf disks treated with all three chemicals showed improved photosynthetic induction at all concentrations compared with the control group (Fig. 3A, B, C). It was also observed that A1N and A4N at high concentrations (4 μg ml^{-1}) would cause significant decreases in Fv/Fm after light stress treatment (Fig. 3D), but leaf disks treated with ANTQ showed significantly lower Fv/Fm at most concentrations except for 0.08 μg ml^{-1} (Fig. 3D). The T_{50} (the time to reach half of the maximum value) of Y(II) in photosynthetic induction showed obvious concentration-dependence behavior in which the Y(II) of the leaf disks treated with high concentrations of chemicals reached plateaus faster than those treated with low concentrations (Fig. 3E). It was also observed that leaf disks treated with A1N showed faster photosynthetic induction at lower concentrations compared with A4N and ANTQ (Fig. 3F).

Electron-accepting abilities of A1N and A4N
Due to the quinone structure of the 9,10-anthraquinone backbone and the similar results of the chemicals groups and the PPB group for
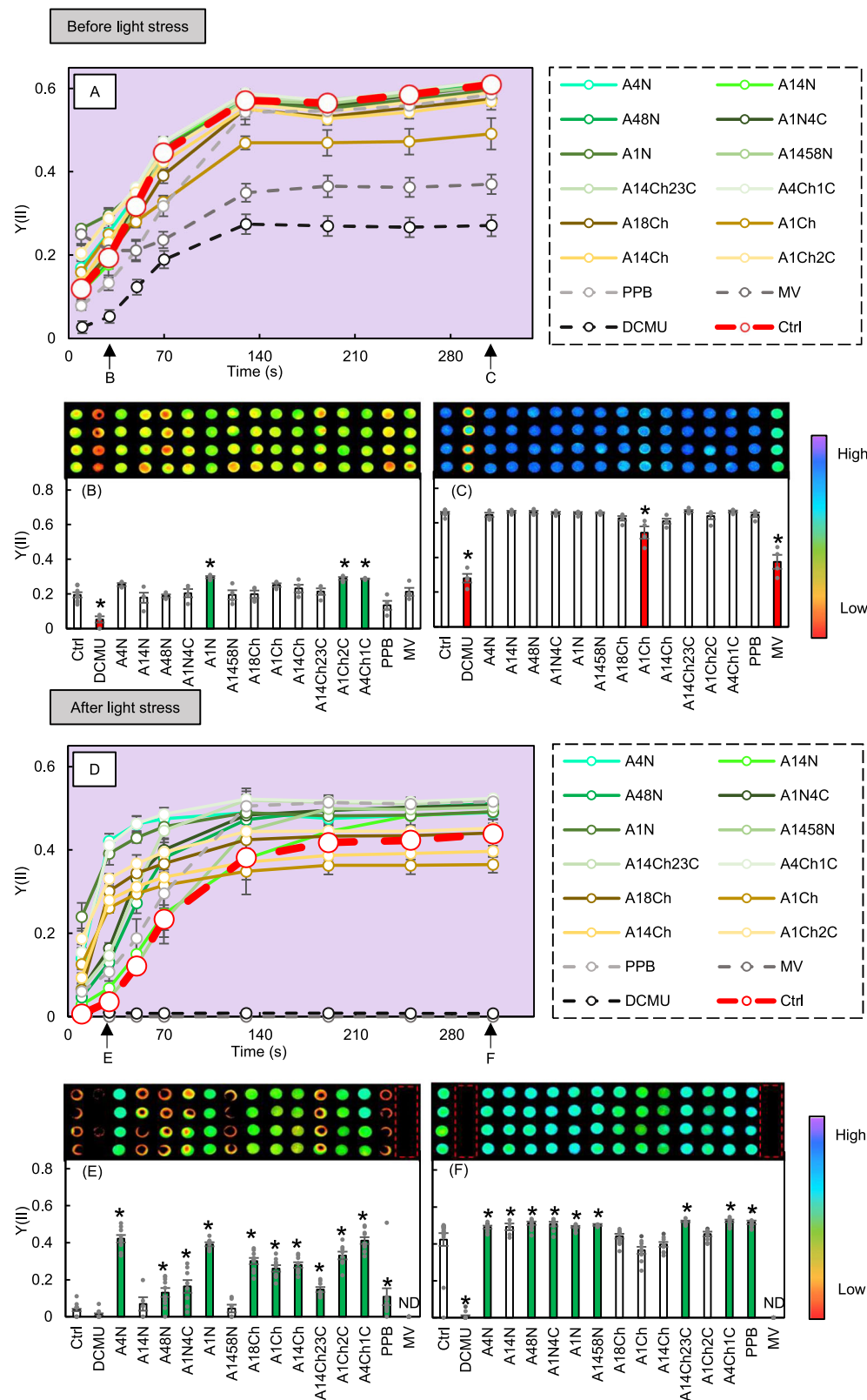
Fig. 2 | Photosynthesis induction curve of chemically treated leaf disks before and after light stress treatment. A Photosynthesis induction curve of chemically treated leaf disks before light stress treatment, with actinic light being 200 µmol m^{-2} s^{-1}. The arrows on the left and right sides indicate data shown in (B), (C). The bold dotted line is the control group. B, C Y(II) of the chemically treated leaf disks at the initial and steady state of photosynthesis induction before light stress treatment. D Photosynthesis induction curve of chemically treated leaf disks after 12 h of light stress treatment, with actinic light be 200 µmol m^{-2} s^{-1}. The arrows on the left and right sides indicate data shown in (E), (F). The bold dotted line is the control group. E, F Y(II) of chemically treated leaf disks at the initial and steady state of photosynthesis induction, after light stress treatment. The pseudo-color Y(II) images of (B), (C), (E), and (F) are placed at the top of each corresponding chart. Ctrl control, PPB phenyl-p-benzoquinone, MV methyl viologen, ND not determined. Data is mean ± SE. *$p < 0.05$, the red color indicates means that are significantly lower than the control group. The green color indicates means that are significantly higher than the control group $n = 6$.

Fig. 3 | hotosynthesis inductions of leaf disks treated with various chemicals with different concentrations after 12 h light stress treatment. A, B, C Photosynthesis inductions of leaf disks treated with A1N, A4N, and anthraquinone (ANTQ) with different concentrations after exposure to high light conditions, with actinic light being 200 μmol m^{-2} s^{-1}. **D** Fv/Fm of leaf disks treated with various chemicals with different concentrations after exposure to high light conditions. **E, F** T$_{50}$ of Y(II) in photosynthetic inductions of leaf disks treated with various chemicals with different concentrations after exposure to high light conditions. Ctrl control, ANTQ anthraquinone. Data is mean ± SE. Bars with the same letter are not significantly different $n = 4$.
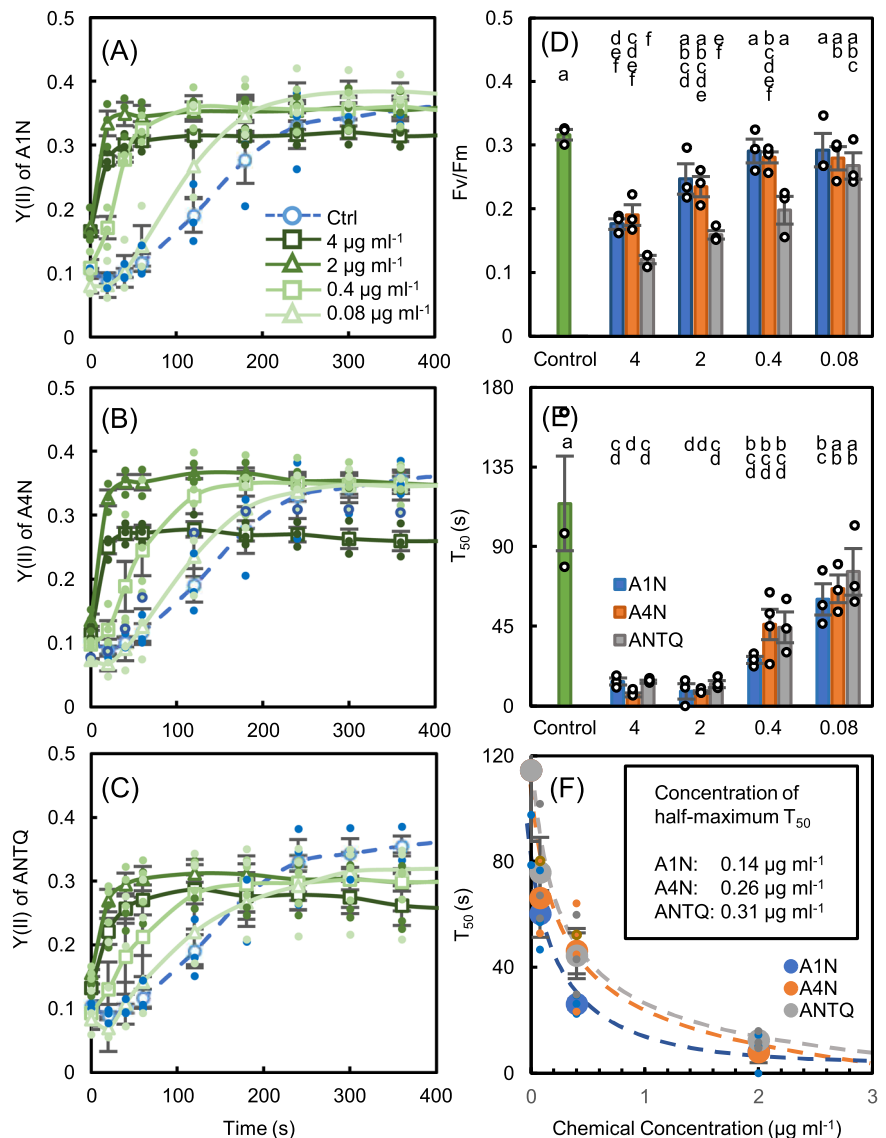
photosynthetic induction, it is possible that these chemicals function by serving as electron acceptors at certain steps of the photosynthetic electron transport chain. Therefore, we determined the electron-accepting ability of A1N and A4N in the photosynthetic electron transport chain because they showed significantly higher Y(II) at both the initial and steady state of photosynthesis during induction after light stress treatment (Fig. 2E, F) and because they also had similar structures (Fig. 1C). In order to evaluate the electron-accepting ability of A1N and A4N, we replaced the PPB or MV with chemicals with the same concentration so that the electron transport rate with chemicals or PPB/MV serving as electron acceptors could be compared.

For measurements of the whole chain electron transport rate, where electron transport from H$_2$O to the donor side of PSI was measured, A1N showed a similar electron-accepting ability as MV, while A4N showed lower electron-accepting ability than MV and A1N (68% of MV) (Fig. 4A). This result also indicated that, based on the principles of this measurement described by Yamasaki et al.[43], A1N and A4N may react with O$_2$ upon being reduced, which is similar to MV. However, electron acceptance by A1N and A4N could happen at any point between PSII and PSI. In order to identify the exact location of electron-accepting, we further measured electron transport at PSII and PSI separately. In measurements of electron transport at PSII, where the electron was transported from H$_2$O to the acceptor side of PSII, the electron accepting ability of A1N and A4N was not detected

(Fig. 4B). In measurements of electron transport at PSI, where the electron was transported from DCPIP to the acceptor side of PSI, A1N and A4N showed lower but obvious electron accepting abilities compared with MV (A1N was 86% and A4N was 78% of MV) (Fig. 4C). These results indicate that A1N and A4N could serve at least partially as electron acceptors from PSI, but not from PSII.

The short-term effects of chemicals on Photosynthetic characteristics in intact leaves

In this study, the effect of chemicals on intact leaves of tobacco, tomato, lettuce, and Arabidopsis were investigated. A1N was chosen for chemical treatment due to its high electron-accepting ability and the high Y(II) value in photosynthetic induction. After light stress treatment, both control groups and A1N treatment groups showed decreases in Fv/Fm, however no significant difference between control groups and A1N treatment groups was observed at each measurement time point in tobacco and lettuce (Fig. 5A, D). Meanwhile, significant decreases of Fv/Fm in control groups compared with A1N treatment groups were observed in tomato and Arabidopsis after 24 h (Fig. 5C, E). Chlorophyll fluorescence was also determined simultaneously with gas exchange. The ETR II and CO$_2$ assimilation rates of tobacco and lettuce showed significant declines in control groups especially after 72 h of light stress treatment, while not in A1N treatment groups (Fig. 5A, C). In tomato and Arabidopsis, A1N treatment increased
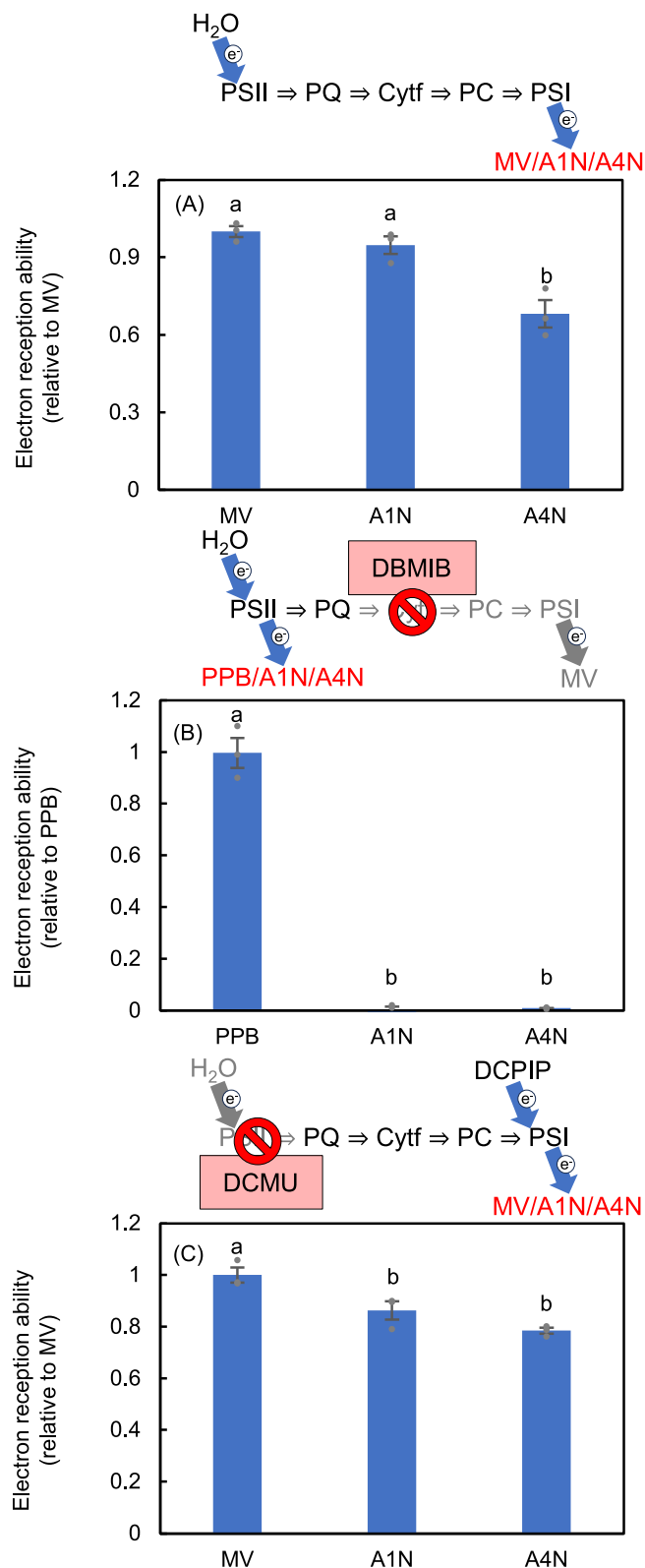
Fig. 4 | Electron reception ability of A1N and A4N compared with methyl viologen (MV) and phenyl-p-benzoquinone (PPB) in whole chain PSII and PSI electron transport measurements. A The electron reception ability of A1N and A4N is compared with MV in the whole-chain electron transport measurement. The electron reception of MV is normalized as 1. **B** The electron reception ability of A1N and A4N is compared with PPB during PSII electron transport measurement. The electron reception of PPB is normalized as 1. **C** The electron reception ability of A1N and A4N is compared with MV during PSI electron transport measurement. The electron reception of MV is normalized as 1. The electron transport pathway of each measurement is indicated above in the corresponding chart. Data is mean ± SE. Means with different letters are significantly different $n = 4$.

were observed in the control group and the A1N treatment group, but no significant difference was observed between them at each measurement time point (Fig. S2A, S2B, S2C, and S2D). In contrast, tobacco leaves treated with A1N showed no significant difference in Fv/Fm and CO_2 assimilation rates compared with the control group with the absence of strong light treatment (Fig. S3). After 72 h of light stress treatment, decreases in leaf greenness, especially in the control group, were observed (Fig. 5A, D), and the chlorophyll concentrations of control groups were significantly lower than A1N treatment groups in tobacco and lettuce (Fig. 5A, D). However, such changes were not observed in tomato (Fig. 5C).

A Dual-PAM-100 was used to investigate the impact of light stress on PSII and PSI in tobacco leaves. After exposure to light stress at 700 µmol photons $m^{-2} s^{-1}$ for 72 h, the ETR II and Y(II) of the A1N treatment group were significantly higher than the control group (Fig. 5B), especially for high light conditions (400–1500 µmol photons $m^{-2} s^{-1}$). However, the Y(NPQ) and Y(NO) of the control group and the A1N treatment group showed only minor differences (Fig. 5B). For PSI activities, the ETR I and Y(I) of the A1N treatment group were significantly higher than the control group at high light conditions (higher than 800 µmol photons $m^{-2} s^{-1}$) (Fig. 5B). Such differences could be explained by significantly lower Y(NA) in the A1N treatment group (Fig. 5B). However, there was no difference between the A1N treatment group and the control group for Y(ND) (Fig. 5B).

The long-term effects of chemicals on the photosynthetic and growth characteristics of Arabidopsis and lettuce

To investigate the long-term effects of chemicals on plant recovery and growth after light stress treatment, the effects of the chemicals on whole Arabidopsis, lettuce and tomato plants were investigated. For Arabidopsis, although no significant differences in Fv/Fm were observed during this stage, the A1N treatment group showed higher Y(II) and lower Y(NPQ) and Y(NO) compared with the control group after 96 h of light stress treatment, at actinic light of cultivation levels and strong light stress levels (Fig. 6A, B). Similar results were observed in lettuce and tomato as well. Higher Y(II) at actinic light of both cultivation and strong light stress levels were also observed in lettuce and tomato (Fig. 7A, B and Fig. 8A, B). In lettuce, lower Y(NPQ) and Y(NO) were observed in the A1N treatment group at both actinic light levels (Fig. 7A, B). In tomatoes, lower Y(NPQ) was observed in the A1N treatment group at actinic light of cultivation level (Fig. 8A, B). Noteworthy, in tomato, the A1N treatment group showed higher Fv/Fm after 96 h of light stress treatment (Fig. 7A, B).

To investigate the effect of the A1N treatment on global transcriptional responses toward high light stress in whole Arabidopsis plants, RNA-seq analysis was conducted. A total of 76 genes were identified as differentially expressed genes (DEGs) between the A1N treatment group and the control group, of which 37 genes were up-regulated and 39 genes were down-regulated in the control group (Table S1). GO enrichment analysis of the DEGs showed that several GO terms that were related to photosynthesis were enriched (Fig. S6A). Therefore, we further examined the expression of the gene encoding photosynthesis apparatus and carbon fixation (Fig. S6B and Table S2). Some genes related to the light-harvesting chlorophyll protein complex, the electron transport chain, and the carbon fixation were slightly down-regulated in the control group compared with the A1N treatment group.

ETR II and CO_2 assimilation rates after 24 and 72 h of light stress, compared to control groups, which generally exhibited lower values for these parameters (Fig. 5D, E). To investigate whether the variations in ETR II and CO_2 assimilation rates were caused by variations in the CO_2 transport rate involved in stomatal gas exchange, we further analyzed the stomatal conductance and intercellular CO_2 concentrations. Declines in stomatal conductance and intercellular CO_2 concentrations after light stress treatment
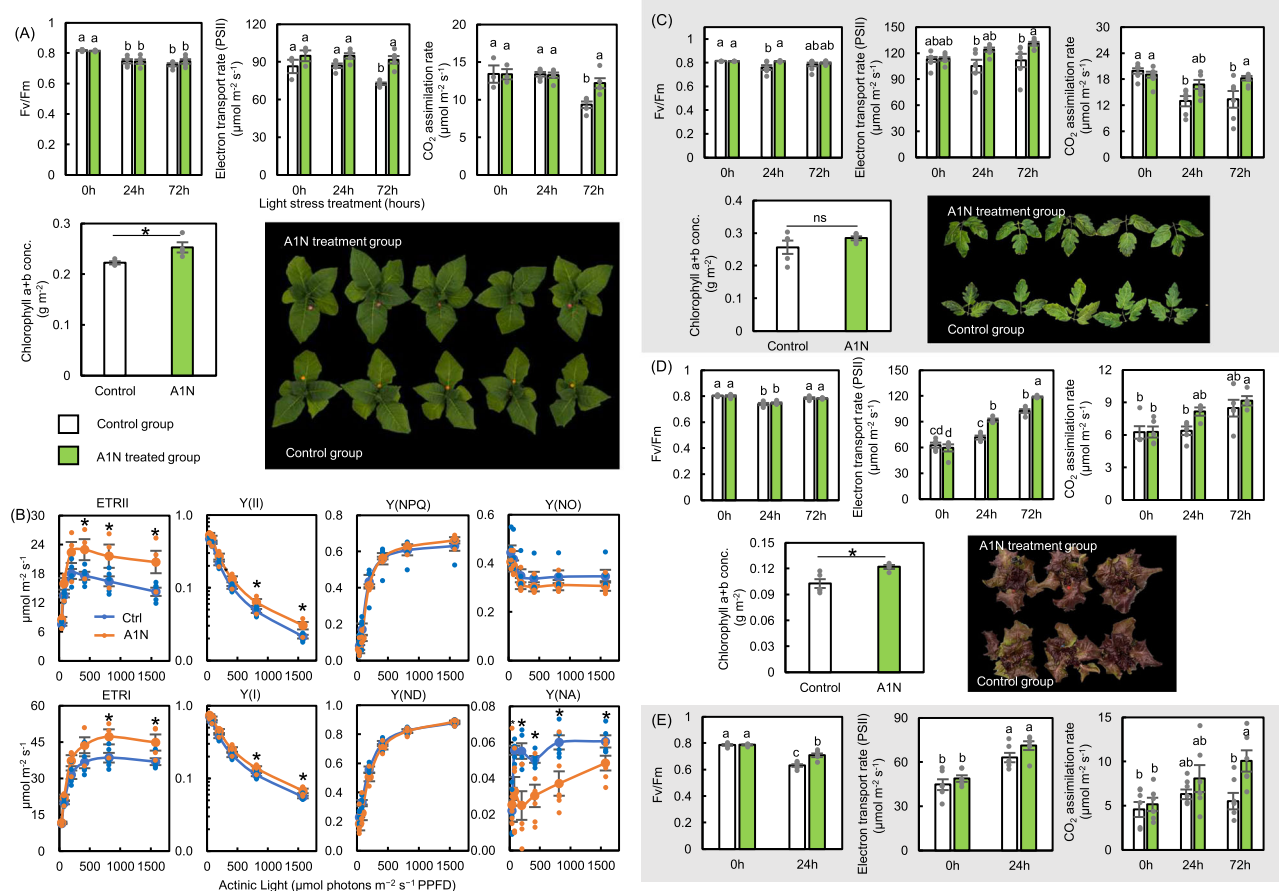
Fig. 5 | Photosynthesis parameters of tobacco, tomato, lettuce, and Arabidopsis leaves after light stress treatment. A Fv/Fm, Electron transport rate of PSII, and CO_2 assimilation rate of tobacco leaves after 0 h, 24 h, and 72 h of light stress treatment. Together with concentration of chlorophyll a + b after 72 h of light stress treatment and Tobacco plants after 72 h of light stress treatment. The leaves of the A1N group were marked with pink stickers, and the leaves of the control group were marked with yellow stickers. **B** Electron transport rate, Y(II), Y(NPQ), Y(NO) of PSII in tobacco leaves after 72 h of light stress treatment. Together with the electron transport rate, Y(I), Y(ND), Y(NA) of PSI in tobacco leaves after 72 h of light stress treatment. **C, D, E** Fv/Fm, Electron transport rate of PSII, and CO_2 assimilation rate of tomato, lettuce, and Arabidopsis leaves after 0 h, 24 h, and 72 h of light stress treatment. Together with the concentration of chlorophyll a + b after 72 h of light stress treatment and leaves after 72 h of light stress treatment (Arabidopsis not included). Ctrl control. Data is mean ± SE. Means with different letters are significantly different. ns $p > 0.05$, *$p < 0.05$, $n = 5$.

After the light stress treatment, plants were restored to the condition of non-stressful cultivation. After 1 week's recovery, plants in control groups showed inhibited growth in all species and early flowering in Arabidopsis, while plants in A1N treatment groups showed almost no sign of such stress (Figs. 6C, 7C, and 8C). Significantly lower Fv/Fm, plant fresh weight, and dry weight were observed in control groups of all species (Figs. 6D, 7D, and 8D). While higher chlorophyll concentrations (SPAD values) were detected in the control group for Arabidopsis (Fig. 6D), the A1N treatment groups for lettuce and tomato showed increased chlorophyll concentrations (Figs. 7D and 8D). Additionally, by the end of the recovery period, anthocyanin concentrations (ACI values) were higher in control groups across all species compared to the A1N treatment groups (Figs. 6D, 7D, and 8D).

Discussion

By performing chemical screening with our system (Fig. 1A), several anthraquinone derivatives with protective effects against light stress were discovered (Fig. 1C). Tobacco leaf disks, intact leaves, and whole Arabidopsis plants treated with the chemical A1N showed improved photosynthesis, and plant growth during and after light stress treatment (Figs. 2, 3, 5, and 6). The electron-accepting ability around the PSI was observed for A1N and A4N (Fig. 4). Therefore, the protective effect of these anthraquinone derivatives can be explained by their ability to

remove excess electrons from PSI. Moreover, it should be noted that the A1N treatment showed no negative effect on plants in non-stress conditions, and intact tobacco leaves treated with A1N showed no significant difference in photosynthesis compared with the control group when continually kept in cultivation conditions (Fig. S3).

Anthraquinone derivatives may serve as electron acceptors
Anthraquinone derivatives are groups of chemicals with robust electrochemical and photochemical activities[44,45]. It was noticed that phenyl-p-benzoquinone, which is an electron acceptor on the donor side of PSII, showed similar but lower protective effects for leaf disks after light stress (Fig. 2). Therefore, it is reasonable to suspect that the protective effect of anthraquinone derivatives is related to their electron-accepting ability as quinones. In order to prove this, electron transport in the isolated thylakoid membrane was measured with an oxygen electrode-based determination system. According to the results of the oxygen electrode, the chemicals A1N and A4N showed similar electron-accepting abilities compared to MV around PSI but not PSII (Fig. 4). This is also explained by the differences in the reduction potentials of A1N, PSI, and PSII. According to previous studies, the reduction potential of A1N is −816 mV vs. the standard hydrogen electrode (the first reduction feature)[46] is lower than MV (−446 mV) but higher than the reduced P700 (−1320 mV) in PSI[47,48] (Fig. S4). However, the redox potential of reduced
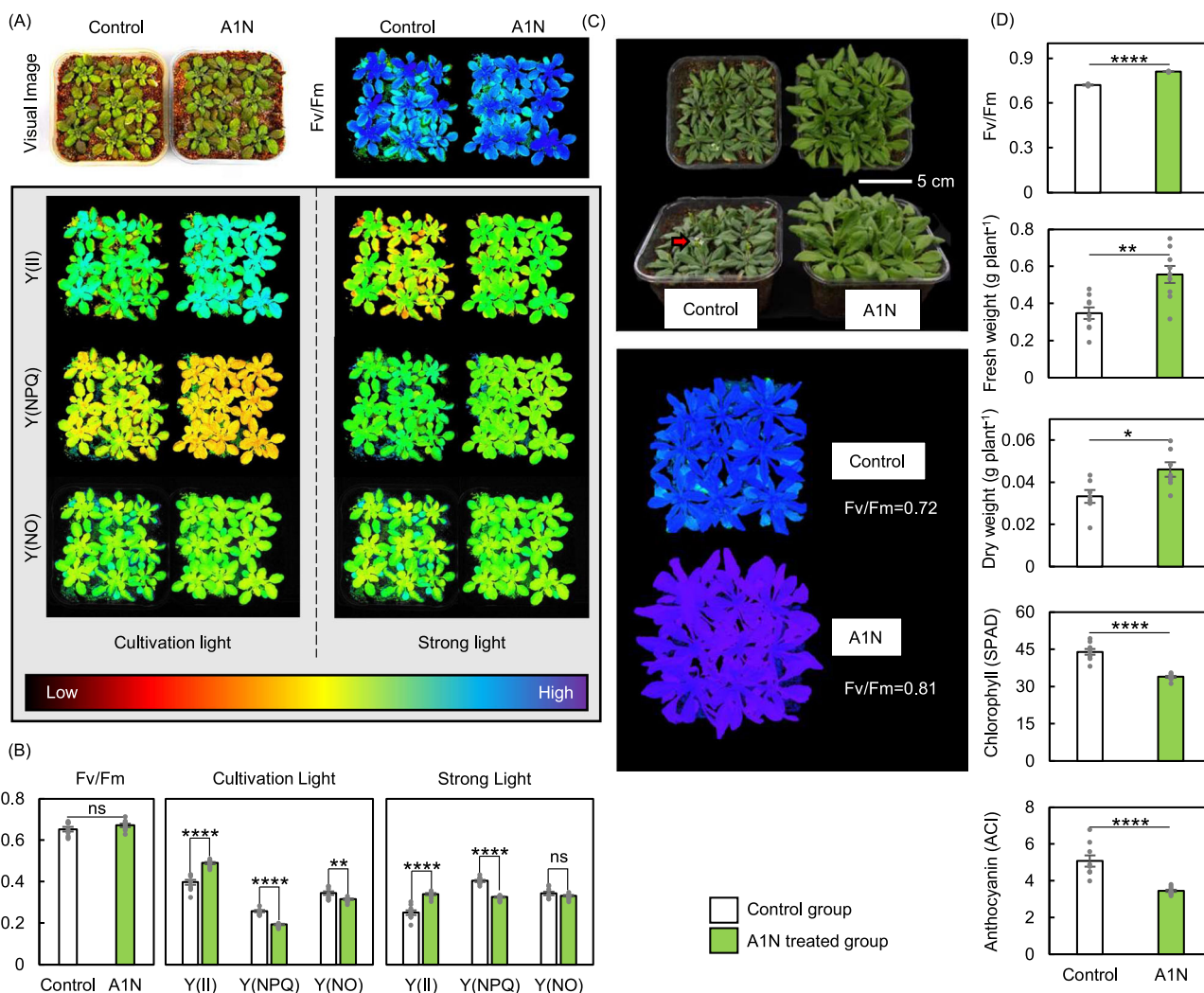
Fig. 6 | Arabidopsis after exposure to light stress for 96 h and 1 week's recovery. **A**, **B** The visual images, pseudo-color (indexed color mode) images, and data of Fv/Fm, Y(II), Y(NPQ), and Y(NO) of plant exposed to light stress for 96 h, under actinic light at cultivation levels (200 μmol photons $m^{-2} s^{-1}$) and strong light stress levels (700 μmol photons $m^{-2} s^{-1}$). **C** The visual images and pseudo-color (indexed color mode) images of the Fv/Fm of plants after 1 week's recovery. The red arrow points to early bloating. **D** Fv/Fm, above ground fresh weight, above ground dry weight, the chlorophyll and anthocyanin contents of plants after 1 week's recovery. Data is mean ± SE. ns $p > 0.05$, *$p < 0.05$, **$p < 0.01$, ****$p < 0.0001$, $n = 9$.

P680 in PSII is -620 to -660 mV[48,49], which is too low for A1N reduction (Fig. S4). These results indicate that A1N can be reduced by PSI primary electron acceptors (A0 and A1) (Fig. S4) upon light illumination but not by PSII. Therefore, it is possible that A1N and other anthraquinone derivatives are engaged in the removal of excess electrons from PSI under light stress conditions. This is further corroborated by the increased qP at the initial state of photosynthetic induction before and after light stress treatment (Fig. S1E, I) and decreased Y(NA) during PSI after light stress treatment (Fig. 5B).

It should be noted that the reduction potential of anthraquinone derivatives is largely influenced by other residues connected to the backbone. For A1N, a NH2- residue is connected to the anthraquinone backbone (Fig. 1C). NH2- is an electron-donating residue that increases the reduction potential of A1N by approximately 132 mV compared with anthraquinone (-684 mV)[46]. A1N and A4N have a single electron-donating residue (Fig. 1C) and have shown strong protective effects against light stress in leaf disks (Figs. 2 and 3). However, derivatives with more than one electron-donating residue, such as A14N, A48N, and A14N58N, showed relatively lower protective effects compared with A1N and A4N (Fig. 2), indicating that overly decreasing the reduction potential can have a negative effect.

Although we confirmed that A1N and A4N could serve as electron acceptors in photosynthetic electron transport, details about the electron accepting process are not clear as the electron-accepting ability of A1N and A4N in whole chain measurements did not perfectly match with the PSI measurements (Figs. 4A and 4C). However, it is possible that the final electron sinks for A1N and A4N mediated electron transport is O_2 as they showed strong electron acceptance in the whole chain and PSI electron transport measurements. This was also the case with MV, which reacted with O_2 upon electron acceptance and reduced O_2 into superoxide. Therefore, electron transport can be detected by investigating the O_2 consumption rate in the solution. As a side effect, MV can cause drastic cell death due to the accumulation of toxic superoxide, especially around the iron-sulfur center of PSI, inducting the Fenton reaction, which could damage the iron-sulfur center of PSI[50]. However, it is not surprising that this effect turned out to be absent in most anthraquinone derivatives we studied. This is because the reaction between anthraquinone derivatives and O_2 upon reduction is slightly different with MV. The reaction of anthraquinone, electrons, and O_2 leads to the formation of endoperoxo complex intermediates rather than free radicals like superoxide, and these intermediate compounds eventually turn into H_2O_2[51] possibly at more distant locations from the iron-sulfur center of PSI (Fig. S4). Therefore, although O_2
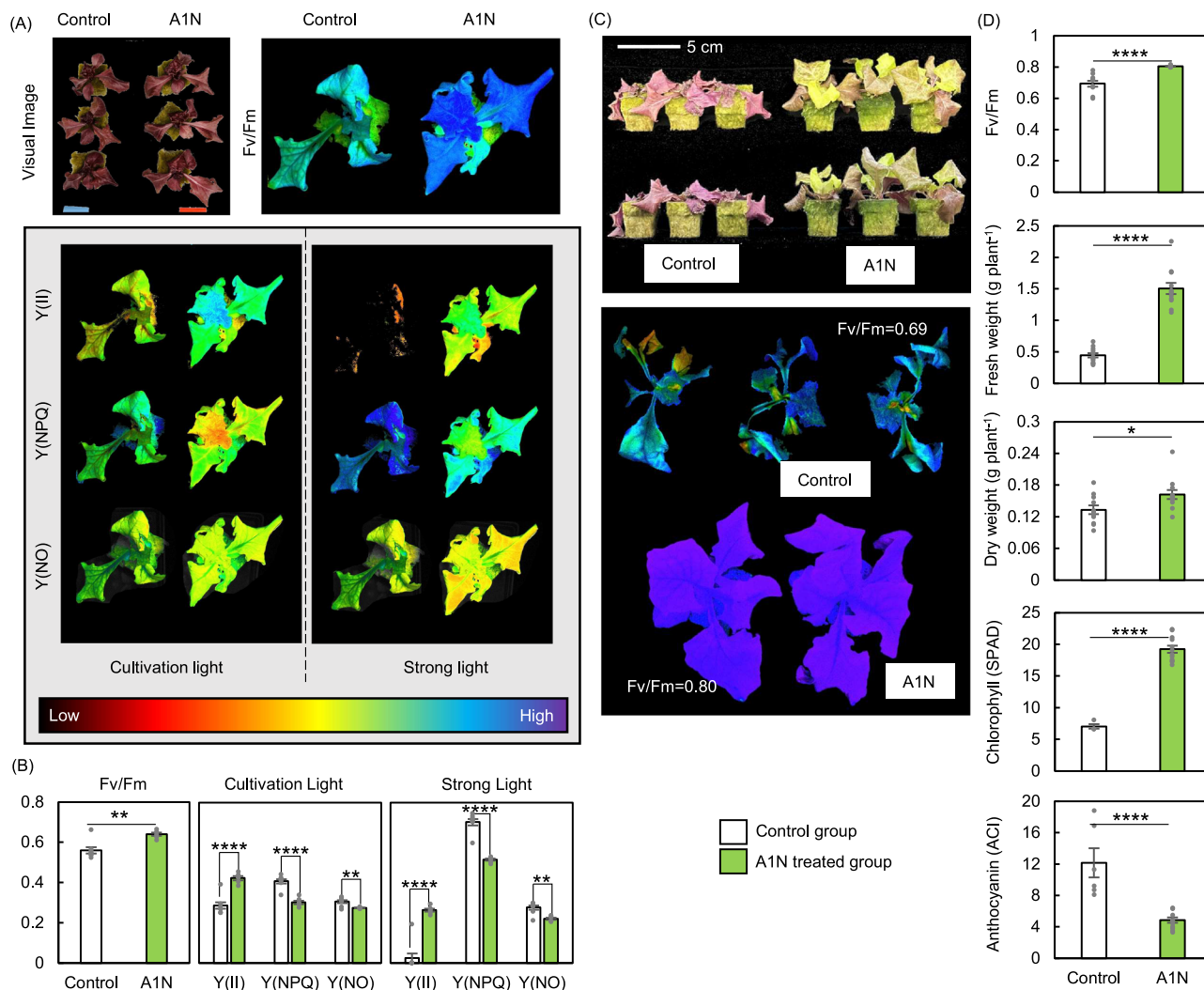
Fig. 7 | Lettuce after exposure to light stress for 96 h and 1 week's recovery.
A, **B** The visual images, pseudo-color (indexed color mode) images, and data of Fv/Fm, Y(II), Y(NPQ), and Y(NO) of plant exposed to light stress for 96 h, under actinic light at cultivation levels (200 μmol photons $m^{-2}\,s^{-1}$) and strong light stress levels (700 μmol photons $m^{-2}\,s^{-1}$). **C** The visual images and pseudo-color (indexed color mode) images of the Fv/Fm of plants after 1 week's recovery. **D** Fv/Fm, above ground fresh weight, above ground dry weight, the chlorophyll and anthocyanin contents of plants after 1 week's recovery. Data is mean ± SE. ns $p > 0.05$, * $p < 0.05$, ** $p < 0.01$, **** $p < 0.0001$, $n = 9$.

serves as a main electron sink for anthraquinone derivatives, this process can be less lethal than reactions between other electron acceptors, such as MV or O_2 only, because the H_2O_2 around the PSI iron-sulfur center could be much lower.

Anthraquinone derivatives improve photosynthesis and growth during and after light stress

In leaf disks, improved photosynthetic induction and higher initial state qP were observed before and after light stress treatment (Fig. 2 and S1), indicating that these chemicals could improve the quantum yield of PSII by providing a higher oxidation state of the primary donor P700 of PSI at the very beginning of photosynthetic induction. For tobacco and tomato leaves, photosynthetic activities were well preserved throughout light stress treatment in A1N treatment groups but decreased significantly in control groups (Fig. 5A, C). In lettuce and Arabidopsis, photosynthetic activities generally increased throughout light stress treatment, which was possibly a result of the plant's acclimation to changing light conditions. Even so, A1N treatment groups showed higher values compared with control groups in this process (Fig. 5D, E). Moreover, such changes in photosynthesis are not likely to be induced by CO_2 concentrations. Although light-induced stomatal closure was observed in light stress

treatments, no significant differences in intercellular CO_2 concentrations and stomatal conductance were observed between the control group and the A1N treatment group (Fig. S2). For whole plants, A1N-treated plants showed higher Fv/Fm and Y(II) and lower Y(NPQ) and Y(NO) with better recovery and fewer signs of stress (Figs. 6, 7, and 8), while the control group showed lower Fv/Fm and higher accumulation of anthocyanin together with inhibited growth and early flowering, which is considered to be a sign of stress factors (Figs. 6, 7 and 8)[52]. It has been reported that the genes encoding the photosynthesis apparatus are repressed during high light stress to mitigate excess absorbed light[53]. In this study, A1N-treated plants showed suppression of some photosynthesis-related gene expressions compared with the control group (Fig. S6). These results suggest that A1N maintained photosynthesis capacity during high light stress by protecting the photosynthetic apparatus from excess light in the transcription levels.

Previous studies have shown that some anthraquinone derivatives may serve as a PSII inhibitor by competing over the QB site on D1-proteins due to their similarity with plastoquinone and that this causes negative effects in electron transport and plant photosynthesis in the short term[54,55]. However, no significant decrease in Fv/Fm was observed in most of the chemical treatment groups for the leaf disks (Fig. S1A and S1B) and tobacco leaves
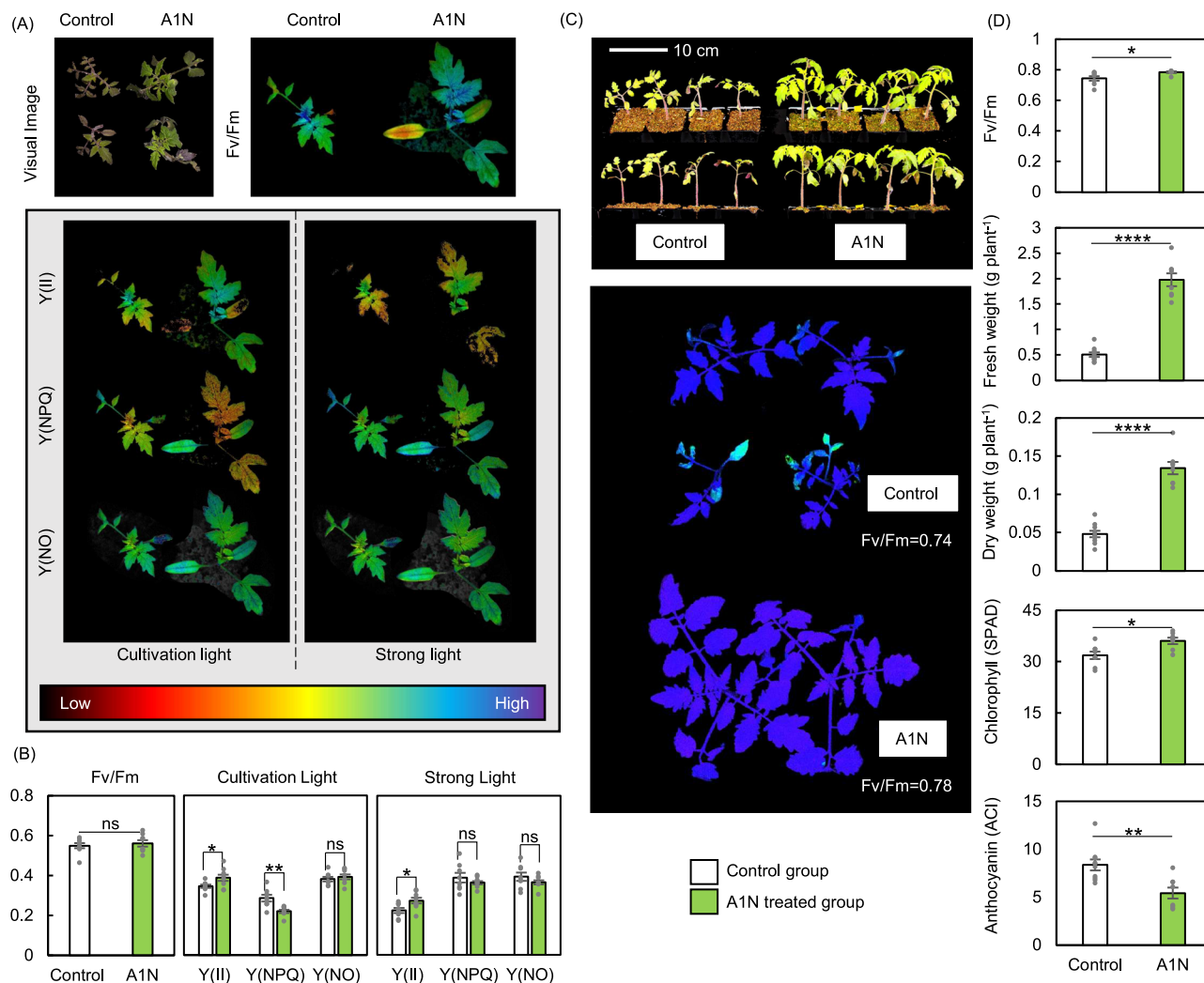
Fig. 8 | Tomato after exposure to light stress for 96 h and 1 week's recovery.
A, **B** The visual images, pseudo-color (indexed color mode) images, and data of Fv/Fm, Y(II), Y(NPQ), and Y(NO) of plant exposed to light stress for 96 h, under actinic light at cultivation levels (200 µmol photons m^{-2} s^{-1}) and strong light stress levels (700 µmol photons m^{-2} s^{-1}). **C** The visual images and pseudo-color (indexed color mode) images of the Fv/Fm of plants after 1 week's recovery. **D** Fv/Fm, above ground fresh weight, above ground dry weight, the chlorophyll and anthocyanin contents of plants after 1 week's recovery. Data is mean ± SE. ns $p > 0.05$, *$p < 0.05$, **$p < 0.01$, ****$p < 0.0001$, $n = 9$.

(Fig. 5A and S3) with or without light stress treatment, and it was only observed in A1N and A4N when the concentrations were very high (4 µg ml^{-1}) (Fig. 3D). This difference is possibly caused by variations in treatment concentrations. In studies mentioned above, anthraquinone derivatives up to 50 µM were applied directly onto separated thylakoid membranes, while in our study, 20–40 µM (2–4 µg ml^{-1}) of anthraquinone derivatives were applied to the outer surface of plant materials and left to diffuse into chloroplasts naturally. Therefore, although the treatment concentrations in studies by Strotmann et al.[54] ($I_{50} = 25$ µM) were similar to those in this study for tobacco leaf disks, and intact leaves, the final concentrations of anthraquinone derivatives presented in chloroplast could be two orders lower in the case of this study (~0.2 µM). When high concentrations (50 µM) of A4N together with MV or PPB were applied directly to thylakoid membranes, significant decreases in thylakoid membrane electron transport rates at whole chain and PSII were observed (Fig. S5A and S5B). These results show that PSII inhibition can be significantly induced by high concentrations of anthraquinone derivatives, as indicated by Strotmann et al.[54]. With lower concentrations, A1N and several other anthraquinone derivatives can protect plants from light stress, improve photosynthesis during light stress, and result in better post-stress recovery, but at higher concentrations, they can also inhibit PSII functions.

Treating plants with certain chemicals to achieve higher tolerances against stresses is a well-explored strategy with many exciting achievements. Over the past decades, there has been increasing evidence that plants can be sensitized for more rapid or more intense mobilization of resistance systems, leading to enhanced tolerance against biotic and abiotic stresses[56]. The physiological state in which plants are able to activate defense responses faster or better is called the primed state of the plant. The use of chemicals to induce the primed state is an interesting topic not only as a mechanism for fundamental research but also for practical applications[40,56]. However, the engagement of stress-response genes in primed state plants results in inhibited growth or reduced photosynthesis, so there is no benefit if there is no stressor[57]. Therefore, a precise prediction of stress conditions is necessary, and plants must be treated at the right time before the stressor fully benefits from the priming effect, which is very difficult to achieve in practical applications. However, in this study, no decrease in photosynthesis was observed in A1N-treated tobacco in non-stressful light conditions (Fig. S3A, B), and no decrease in dry weight was observed in tomato plants (Fig. S3C, D). This indicates that we can treat plants with chemicals, such as A1N, to prevent light stress at any time without worrying about the negative effects.

It is also worth noticing that cultivation conditions used in our study, especially light conditions, were not stressful for plant materials studied in this research, although they are generally weaker (around 150 μmol photons m^{-2} s^{-1}) compared with natural light conditions in agricultural production. As indicated by our results, tobacco kept at cultivation conditions showed Fv/Fm of around 0.8 (Fig. S3), similar results could also be observed in tomatoes, lettuces, and Arabidopsis (Figs. 6–8), as plants restored to cultivation conditions showed Fv/Fm of around 0.8 in well-recovered leaves. Previous studies showed that Fv/Fm in healthy, non-stressed plants typically falls within the range of 0.79 to 0.84[58]. Thus, the plant materials used in our study are well-suited to represent plant responses to light stress and chemical treatments, despite the relatively lower light intensity in the cultivation setup.

Anthraquinone derivatives can be used as agrochemicals

Anthraquinone derivatives are widely found in natural environments. In lichen, they have been found to provide protection against UV-B damage[59], and they are present in rhizomes, flowers, and fruits. More than 200 compounds belonging to these derivatives were identified in plants. They play various roles, such as the regulation of energy transfer and cell death[60]. Due to their wide range of colors, anthraquinone derivatives are used as dyes in industry[61]. They are also well known for their anticancer, anti-inflammatory, diuretic, anti-arthritic, antifungal, antibacterial, and antimalarial properties[60]. They are also used in many traditional herbal medicines to cure digestive system disorders[62]. Some anthraquinone derivatives have been used for nonlethal pest management in agricultural production since the 1940s[63]. To confirm the safety issue in agricultural applications, especially on edible parts of plants, we determined the persistence of anthraquinone derivatives. The results showed that such chemicals experienced a quick decay process after surface application, and became undetectable within 7 days of normal cultivation (Fig. S7).

In organisms, there are two major pathways that are engaged in the synthesis of anthraquinone chemicals. The first is the polyketide pathway, which is observed in *Photorhabdus luminescens*, a gammaproteobacterium of the family Morganellaceae. It is a lethal pathogen of insects and higher plants, including *Senna tora*[64,65]. In this pathway, octaketide is dehydrated, and several anthraquinone derivatives, including Endocrocin, Physcion, Rhein, and Chryso-obtusin, are synthesized[65]. The second pathway is a combination of shikimate and mevalonate/methyl-D-erythritol 4-phosphate pathways, which is observed in *Cinchona officinalis* and *Rheum tanguticum*[66,67]. In this pathway, products from the Shikimate and Terpenoid pathways, including shikimic acid, glucose, acetyl CoA, pyruvate, and glyceraldehye 3-P, are further processed to synthesize anthraquinone derivatives[66]. Although these two pathways have not been found in Arabidopsis or tobacco, it would be an interesting avenue of research to verify whether these two pathways for anthraquinone biosynthesis are also functional in Arabidopsis, tobacco, and other crop plants and whether it is possible to introduce anthraquinone synthesis pathways into these plants. If it is, it could result in the natural accumulation of such chemicals within plant cells and provide them with endogenous protection against light stress. However, the detailed biosynthesis of anthraquinone is still unclear for plant species. According to previous studies in *Rheum tanguticum* and *Senna tora*, a total of more than 200 candidate enzyme genes are involved in the synthesis of anthraquinone[66,67], and it is hard to tell which of them are essential for the introduction of anthraquinone synthesis pathways in other plants. So further studies are required.

In this study, A1N showed significant protective effects against light stress in tobacco, lettuce, tomato, and Arabidopsis (Figs. 2, 3, 5, 6, 7, 8) with no negative effects in non-stressful conditions (Fig. S3). Moreover, there was no data suggesting that A1N is toxic. Therefore, A1N or A1N analogs are candidate compounds for the development of light stress protectors in agriculture. Utilization of these chemicals for enhanced light stress tolerance offers a new method for securing the productivity of food crops and the commercial benefits of high-value products, including fruits, vegetables, flowers, herbs, and ornamental plants, under extreme light intensities. Hopefully, these findings will inspire the development of new techniques that enhance the tolerance of plants in order to address the challenges of this unprecedented period of global climate change.

Materials and methods
Chemical library and compounds
A total of 12,000 compounds from the chemical library provided by Maybridge Chemical Company Limited were used in the screening together with 10 structural analogs, the photosynthesis inhibitor DCMU, the electron receptor phenyl-p-benzoquinone (PPB), and Methyl viologen (MV) (Fig. 1C). Structural analogs were obtained from the database of ChemCupid. All chemicals were diluted with DMSO to a stock concentration of 2 mg ml^{-1} and kept at −80 °C.

Plant materials and growth conditions
Tobacco (*Nicotiana tabacum* L. "Wisconsin-38"), Arabidopsis (*Arabidopsis thaliana* (L.) Heynh., "Columbia-0 (CS60000)"), tomato (*Solanum lycopersicum* L. "CF Chika") and lettuce (*Lactuca sativa* L. "New Red Fire Lettuce") were used in this study. The seeds of tobacco and Arabidopsis were sown in a 1:1 mixture of MetroMix (Metromix 350, Hyponex) and vermiculite. Lettuce was sown on rockwool. All plants were cultivated in a temperature-controlled growth chamber for the first 3–4 weeks. The growth chamber was operated with a daylight/dark period of 10/14 h, and PPFD in the daylight period was set to 150 μmol photons m^{-2} s^{-1}. Air temperature and relative humidity were set to a constant 22 °C and 60%, respectively. Arabidopsis, tomato, and lettuce cultivated in the growth chamber were used for experiments in the third week. After four weeks, tobacco plants were transplanted into φ252×300 mm pots with 100% Akadama soil (red granular soil) in a greenhouse, and 5 g of full nutrition fertilizer (A906, JCAM AGRI. CO., LTD.) was applied to each pot. Fully expanded tobacco leaves after 8–12 weeks (before the flowering stage) of cultivation were harvested for further measurements. The spinach (*Spinacia oleracea*) used in this study was purchased at a local retail store.

Construction of a chemical screening system using tobacco leaf disks
To ensure highly efficient screening of large amounts of chemicals, a system of 96-well plates loaded with leaf disks in each well was constructed (Fig. 1A). Tobacco plants cultivated for 8–12 weeks were moved to a dark room 24 h before the experiment. Leaf disks were collected from fully expanded leaves with a leaf punch (φ = 5.35 mm). To ensure the homogeneity of photosynthesis properties, only healthy leaf tissue that was not adjacent to leaf veins or the edges of leaves was used. Collected leaf disks were kept in a 96-well plate container for treatment and measurement, and one 7 mm surgical cotton ball was placed in each well of the 96-well plates (Thermo Fisher Scientific). Black plates were used to minimize light reflection and penetration, which could cause noise when taking measurements. 200 μl of distilled water was added to each well to create a moist environment. Leaf disks were placed on the cotton balls with the top side of the leaves facing upward. They were kept wet throughout this process (Fig. 1A).

Chemical components were added to the well of each plate for a final concentration of 2 μg ml^{-1}. Plates loaded with diluted chemicals and leaf disks were vacuum-infiltrated for 5 min, and chlorophyll florescence was then determined with the Imaging-PAM M-Series (IMAGING-PAM; Walz, Effeltrich, Germany) to evaluate the instant effect of the chemicals on photosynthesis. The leaf disks in the plates were then exposed to high light intensity for 12 h; the plates were sealed with cling film to prevent evaporation and placed in a growth chamber operated with a constant light period; and PPFD was set to 700 μmol photons m^{-2} s^{-1}. Air temperature and relative humidity were set to a constant 22 °C and 60%, respectively. After high light treatment, chlorophyll florescence was again determined

with the Imaging-PAM to evaluate the protective effect of the chemicals on photosynthesis against light stress (Fig. 1B).

Each chemical could be applied onto one leaf disk (high throughput but low accuracy) or multiple leaf disks (low throughput but high accuracy). In this study, high throughput screening was used for the first screening of the whole chemical library and low throughput screening was used for the second screening to confirm the results obtained in the first screening. A fully expanded tobacco leaf (major-axis length of over 30 cm) harvested between 8–12 weeks can provide enough leaf disks for approximately four 96-well plates. In this study, eight plates were processed in one day. Therefore, around 700 different chemicals could be tested in a day.

The short- and long-term effects of the chemicals on living plants

The short-term (from hours to days) and long-term effects (from days to week) of the chemicals on the plants were determined separately. For short-term chemical effects, intact leaves from tobacco, tomato, lettuce, and Arabidopsis seedlings cultivated for 3–4 weeks in the growth chamber were used. Leaves (not detached from the plant) were immersed in 4 µg ml^{-1} of chemicals plus 0.2% solvent DMSO (chemical treatment group) or 0.2% DMSO only (control group) for 1 h and then returned to cultivation conditions and kept in the dark for 12 h. For light stress treatments, plants were moved to a growth chamber with the same temperature and relative humidity as the cultivation conditions, but PPFD was at a constant 700 µmol photons m^{-2} s^{-1}. Gas exchange, chlorophyll fluorescence, and P700 redox state in treated leaves were determined with the LI-6400XT (Li-COR, Lincoln, NE), the Imaging-PAM M-Series (Walz, Effeltrich, Germany), and the DUAL-PAM-100 (Walz, Effeltrich, Germany) throughout the light stress treatments. Treated leaves were harvested, and the chlorophyll concentrations of treated leaves were determined after 72 h of light stress treatment.

To analyze the long-term effects of the chemicals, the seedlings of Arabidopsis, tomato, and lettuce cultivated for 3 weeks were used. Plants were sprayed with 20 µg ml^{-1} of chemicals plus 1% solvent DMSO (chemical treatment group) or 1% DMSO only (control group). For light stress treatment, plants were moved to a growth chamber with the same temperature and relative humidity as the cultivation conditions, but PPFD was at a constant 700 µmol photons m^{-2} s^{-1}. Plants were treated with stressful light conditions for 96 h and then returned to cultivation conditions and allowed to recover for 1 week before harvesting. RNAseq of Arabidopsis was determined by the end of the light stress treatment, and chlorophyll fluorescence was determined with the Imaging-PAM throughout the light stress treatment and after 1 week's recovery. The SPAD value, anthocyanin concentration, and above-ground biomass were determined after 1 week's recovery.

Analysis of gas exchange, chlorophyll fluorescence, and P700 measurements

The determination of the electron transport rate during PSII and PSI was conducted with the Maxi-version of the Imaging-PAM M-Series (Walz, Effeltrich, Germany) and the DUAL-PAM-100 (Walz, Effeltrich, Germany). For the chemical screening system for leaf disks, actinic light was set to 64 µmol m^{-2} s^{-1} in the Imaging-PAM system. To ascertain the long-term effects of the chemicals on Arabidopsis, tomato, and lettuce seedlings, actinic light was set to 200 µmol m^{-2} s^{-1} and 700 µmol m^{-2} s^{-1}. The chlorophyll fluorescence from plant materials was selected by defining the areas of interest (AOI) with the ImagingWin Software (Walz), and pseudo-color (indexed color mode) images of tested material could be obtained. For the Dual-PAM-100 measurements, intact leaves were clamped in the 1.4 cm^2 chamber of a gas exchange system (GFS-3000, Walz Germany). To measure the short-term effects of the chemicals on tobacco, tomato, lettuce, and Arabidopsis seedlings, actinic light was set to gradients ranging from 30 to 1600 µmol m^{-2} s^{-1}. To obtain stable fluorescence from the samples, each state lasted for 180 s. The maximum potential photochemical quantum yield of photosystem II (PSII) (Fv/Fm), the effective quantum yield of photochemical energy conversion during PSII (Y[II]), the quantum yield of regulated energy dissipation during PSII (Y[NPQ]), the photochemical quenching of PSII (qP), and the fraction of open PSII centers (qL) was calculated as follows according to Alexander V. Ruban[68]. Y(I), Y(ND), and Y(NA) were estimated according to Klughammer and Schreiber[69]. The electron transport rate (ETR) of PSII and PSI was calculated as ETR I (or ETR II) = $0.5 \times$ abs I $\times$ Y(I) (or Y[II]), where 0.5 is the fraction of absorbed light between PSII and PSI (assuming they are equal), and abs I is absorbed irradiance taken as 0.84 of incident irradiance. All plant materials were kept in the dark for at least 30 min before being measured.

The determination of the CO_2 assimilation rate was conducted with a portable gas exchange system (LI-6400XT, Li-COR, Lincoln, NE). The photosynthetic rate was measured at a PPFD of 500 µmol photons m^{-2} s^{-1}, a CO_2 concentration of 400 µmol mol^{-1}, relative humidity of 60%, and temperature of 25 °C.

Quantifying photosynthetic pigments

To determine chlorophyll concentrations, six-leaf disks were collected from each leaf sample with a leaf punch ($\varphi = 5.35$ mm) after the final harvest. They were then put into an Eppendorf tube containing 1 ml of 80% acetone solution. The chlorophyll was extracted without grinding after being incubated at 4 °C for 48 h. The chlorophyll content was spectrophotometrically analyzed with a Spectrophotometer (Shimadzu, UV-1280) at wavelengths of 663 nm and 646 nm[70]. To determine the above-ground biomass, the above-ground tissue of the plants was harvested, placed in paper envelopes, and dried at 80 °C for 48 h. The dry weight was then determined with an analytical balance. SPAD values were determined with a hand-held SPAD-502 meter (Spectrum Technologies, Inc.). Anthocyanin concentrations were measured with a hand-held Anthocyanin Content Meter (CCM 200 A plus, produced by V S INSTRUMENT PVT. LTD).

Ascertaining the electron-accepting abilities of the chemicals

Thylakoid membranes were prepared from spinach leaves to evaluate photosynthetic electron transport with the presence of chemicals[71,72]. For the preparation of thylakoid membranes, leaves were homogenized in an ice-cold blending buffer (50 mM Hepes-KOH, pH 7.8, 0.33 M sorbitol, 2 mM EDTA, 1 mM MgCl$_2$, 1 mM MnCl$_2$, 25 mM Na-ascorbate, and 1 mM DTT). The homogenate was filtered through a layer of Miracloth (Calbiochem), and the filtrate was centrifuged at $2000 \times g$ for 30 s (s). The supernatant was removed, and thylakoid membranes in the pellet were suspended with a suspending buffer (0.33 M sorbitol and 50 mM Hepes-KOH, pH 7.8). Electron transport activities in the thylakoid membranes (10 µg chlorophyll ml^{-1}) suspended in the medium described above were measured with a Clark-type oxygen electrode (Hansatech, King's Lynn, the UK) in a saturating white LED light, by monitoring the decreases or increases of O$_2$ concentration within the solution as explained by Yamasaki et al.[43]. To measure whole-chain electron transport activity, 5 mM methylamine, 0.5 mM sodium azide, and 50 µM methyl viologen (or 50 µM of chemicals) were added to the suspension. The assay medium for PSI electron transport activity contained 10 mM methylamine, 5 µM DCMU, 0.5 mM sodium azide, 150 µM DCIP, 1 mM sodium ascorbate, and 50 µM methyl viologen (or 50 µM of chemicals). The activity of PSII electron transport was determined with 50 µM of phenyl-p-benzoquinone (or 50 µM of chemicals) as an electron acceptor in the presence of 0.25 µM of 2,5-dibromo-3-methyl-6-isopropyl-p-benzoquinone and 1 µM of DBMIB, with modifications to the method of Yamasaki et al.[43].

RNA extraction and RNA-seq analysis

RNA was extracted from whole Arabidopsis plants after they were exposed to continuous light stress for 96 h by using the RNeasy Plant kit (QIAGEN, Hilden, Germany). The library for RNA-seq was constructed using the protocol of Lasy-Seq[73] ver. 1.1 (https://sites.google.com/view/lasy-seq/) and sequenced using Nova Seq plus (Illumina, San Diego, CA, USA) with single-end sequencing lengths of 150 bp. All obtained raw reads were trimmed using the Trimmomatic ver. 0.33[74] with the following parameters:

ILLUMINACLIP:TruSeq3-SE.fa:2:30:10 LEADING:20 TRAILING:20, SLIDINGWINDOW:4:15 MINLEN:40. The trimmed reads were mapped onto the reference A. thaliana genome (TAIR10; https://ftp.ensemblgenomes.ebi.ac.uk/pub/plants/release-55/fasta/arabidopsis_thaliana/dna/Arabidopsis_thaliana.TAIR10.dna.toplevel.fa.gz) using STAR ver. 2.7.10b[75], and the read counts per gene were calculated using RSEM ver. 1.3.3[76]. Differentially expressed genes (DEGs) between the control group and the chemical treatment group were detected by the criteria of |fold-change| > 1.5 and false discovery rate = 0.1 using the DESeq2 R package ver. 1.40.2[77]. Furthermore, the gene ontology (GO) enrichment analysis of DEGs was implemented by the criteria of adjusted P-value < 0.01 using clusterProfiler R packages ver. 4.8.3[78].

Determination of chemical persistence using GC-MS

To determine the persistence of anthraquinone derivatives within plant materials, GC-MS analysis was conducted. A4Ch1C was used in plant treatment because it is much easier for GC-MS system to quantify compared with A1N, which was applied in most other analyses. Lettuce before chemical application (Day0-Blank), right after chemical application (Day0-Chem), and 7 days after chemical treatment (Day7-Chem) were harvested and homogenized into fine powder in liquid nitrogen. Methanol (MeOH) and the corresponding internal standard (100 μL DMSO solution of A14Ch23C, 1.33 μg) were added to each sample, and then two chemicals (A4Ch1C and A14Ch23C) were extracted using three zirconia beads for 30 s with Shake–Master NEO (BMS, Japan) and repeated six times. After centrifugation at $2000 \times g$ for 6 min, the supernatant was evaporated for 1 h. The remained portion was mixed with 6 mL of 25 mM NH_4HCO_3, and the two chemicals were purified from the mixture with MAX columns (60 mg, 3 cc, Waters, USA) activated with MeOH and pre-equilibrated with 3 mL 25 mM NH_4HCO_3. The samples were washed with 3 mL 25 mM NH_4HCO_3, and the two chemicals were eluted with 3 mL MeOH. Purified samples were evaporated. For gas chromatography-mass spectrometry (GC-MS) analysis, 50 μL MeOH was added to each dried sample. The sample was taken with a syringe (10 μL Microliter Syringes, Hamilton, NV, USA), and a portion (1 μL) was injected into GC-MS. The measurements were performed under the following conditions: instrument, GCMS-QP2010 SE (Shimadzu, Kyoto, Japan); column, DB-1 (15 m × 0.250 mm × 0.25 μm, Agilent Technologies, Santa Clara, CA, USA); carrier gas, He; linear velocity, 83.0 cm s^{-1}; initial column temperature, 120 °C; injection mode, split-less; initial temperature program, 120 °C; temperature program, $0 \rightarrow 2$ min, 120 °C, $2 \rightarrow 4$ min, 120 °C $\rightarrow$ 180 °C (linear-gradient, 30 °C min^{-1}), $4 \rightarrow 14$ min, 180 °C $\rightarrow$ 210 °C (linear-gradient, 3 °C min^{-1}), $14 \rightarrow 16.8$ min, 210 °C $\rightarrow$ 280 °C (linear-gradient, 25 °C min^{-1}), $16.8 \rightarrow 20.8$ min, 280 °C; injector temperature, 250 °C; ion source temperature, 200 °C; interface temperature, 250 °C; ionization mode, EI (70 eV). Equal amounts of A4Ch1C and A14Ch23C were used in advance, and the peak area of m/z 256 for A4Ch1C and the peak area of m/z 306 for A14Ch23C were compared. The quantification of A4Ch1C was performed on the basis of the peak area of A14Ch23C. All tests were basically performed in quadruplicate. A one-way ANOVA with a post-hoc Tukey HSD test was adopted (**0.0021).

Statistical and reproducibility

The significance of variations between multiple means was evaluated by the Tukey–Kramer test. The significance of variations between the two means was evaluated by the Student's t-test. Statistical analysis was performed using Prism v. 8.0.1 software.

All analysis showed in this study contains a sample size of no less than 4 replicates. All replicates are defined from random choice of plant materials from independent individuals.

Reproducibility was ensured through detailed documentation of protocols, including plant growth conditions, data collection, and sample processing techniques. Raw data used in this study are available in the supplementary materials. These resources enable reproducibility and allow independent verification of the findings.

Data availability

Supporting data can be requested by contacting the corresponding author. Raw data could also be found in supplementary materials named as "supplementary data". The raw RNA-seq data were deposited at the National Center for Biotechnology Information (https://www.ncbi.nlm.nih.gov/) under BioProject accession PRJDB17308.

References

1. Rosenzweig, C., Iglesius, A., Yang, X.-B., Epstein, P. R., & Chivian E. Climate Change and Extreme Weather Events-Implications for Food Production, Plant Diseases, and Pests. (University of Nebraska—Lincoln, 2001).
2. Minhas P. S., Rane J., & Pasala R. K. Abiotic Stress Management for Resilient Agriculture (Springer, 2017).
3. Sharma, A. et al. Photosynthetic response of plants under different abiotic stresses: a review. J. Plant Growth Regul. 39, 509–531 (2020).
4. Yamori, W., Makino, A. & Shikanai, T. A physiological role of cyclic electron transport around photosystem I in sustaining photosynthesis under fluctuating light in rice. Sci. Rep. 6, 1–2 (2016).
5. Boonchai, C. et al. Rice overexpressing OsNUC1-S reveals differential gene expression leading to yield loss reduction after salt stress at the booting stage. Int. J. Mol. Sci. 19, 3936 (2018).
6. Kang, L. et al. Suppression of the β-carotene hydroxylase gene increases β-carotene content and tolerance to abiotic stress in transgenic sweetpotato plants. Plant Physiol. Biochem. 117, 24–33 (2017).
7. Mosa K. A., Ismail A. & Helmy M. in Plant Stress Tolerance. 1–19. (Springer, Cham, 2017).
8. Yamori, W., Hikosaka, K. & Way, D. A. Temperature response of photosynthesis in C3, C4, and CAM plants: temperature acclimation and temperature adaptation. Photosynth. Res. 119, 101–117 (2014).
9. Yamori, W. & Shikanai, T. Physiological functions of cyclic electron transport around photosystem I in sustaining photosynthesis and plant growth. Annu. Rev. Plant Biol. 67, 81–106 (2016).
10. Hussain, S. et al. Photosynthesis research under climate change. Photosynth. Res. 150, 5–19 (2021).
11. Qu, Y., Mueller-Cajar, O. & Yamori, W. Improving plant heat tolerance through modification of Rubisco activase in C3 plants to secure crop yield and food security in a future warming world. J. Exp. Bot. 74, 591–599 (2023).
12. Demmig-Adams, B. & Adams, W. W. Photoprotection and other responses of plants to high light stress. Annu. Rev. Plant Physiol. Plant Mol. Biol. 43, 599–626 (1992).
13. Long, S. P., Humphries, S. & Falkowski, P. G. Photoinhibition of photosynthesis in nature. Annu. Rev. Plant Physiol. Plant Mol. Biol. 45, 633–662 (1994).
14. Takahashi, S. & Murata, N. Interruption of the Calvin cycle inhibits the repair of photosystem II from photodamage. Biochim. Biophys. Acta-Bioenerg. 1708, 352–361 (2005).
15. Telfer, A. Singlet oxygen production by PSII under light stress: mechanism, detection and the protective role of beta-carotene. Plant Cell Physiol. 55, 1216–1223 (2014).
16. Endo, T., Shikanai, T., Takabayashi, A., Asada, K. & Sato, F. The role of chloroplastic NAD(P)H dehydrogenase in photoprotection. FEBS Lett. 457, 5–8 (1999).

17. Ishida, S. et al. Diurnal and developmental changes in energy allocation of absorbed light at PSII in field-grown rice. *Plant Cell Physiol.* **55**, 171–182 (2014).

18. Murata, N., Takahashi, S., Nishiyama, Y. & Allakhverdiev, S. I. Photoinhibition of photosystem II under environmental stress. *Biochim. Biophys. Acta (BBA)-Bioenerg.* **1767**, 414–421 (2007).

19. Ilić, Z. S., Milenković, L., Stanojević, L., Cvetković, D. & Fallik, E. Effects of the modification of light intensity by color shade nets on yield and quality of tomato fruits. *Sci. Horticulturae* **139**, 90–95 (2012).

20. Allahverdiyeva, Y., Suorsa, M., Tikkanen, M. & Aro, E. M. Photoprotection of photosystems in fluctuating light intensities. *J. Exp. Bot.* **66**, 2427–2436 (2015).

21. Van Rooijen, R. et al. Natural variation of YELLOW SEEDLING1 affects photosynthetic acclimation of *Arabidopsis thaliana*. *Nat. Commun.* **8**, 1–9 (2017).

22. Li, X. et al. Maize GOLDEN2-LIKE genes enhance biomass and grain yields in rice by improving photosynthesis and reducing photoinhibition. *Commun. Biol.* **3**, 1–12 (2020).

23. Davison, P. A., Hunter, C. N. & Horton, P. Overexpression of β-carotene hydroxylase enhances stress tolerance in Arabidopsis. *Nature* **418**, 203–206 (2002).

24. Emiliani, J., Grotewold, E., Ferreyra, M. L. & Casati, P. Flavonols protect Arabidopsis plants against UV-B deleterious effects. *Mol. Plant* **6**, 1376–1379 (2013).

25. Ksas, B., Becuwe, N., Chevalier, A. & Havaux, M. Plant tolerance to excess light energy and photooxidative damage relies on plastoquinone biosynthesis. *Sci. Rep.* **5**, 1–6 (2015).

26. Lee, H. Y. & Back, K. Melatonin induction and its role in high light stress tolerance in *Arabidopsis thaliana*. *J. Pineal Res.* **65**, e12504 (2018).

27. Götz, T., Sandmann, G. & Römer, S. Expression of a bacterial carotene hydroxylase gene (crtZ) enhances UV tolerance in tobacco. *Plant Mol. Biol.* **50**, 127–140 (2002).

28. Basso, L., Sakoda, K., Kobayashi, R., Yamori, W. & Shikanai, T. Flavodiiron proteins enhance the rate of CO2 assimilation in Arabidopsis under fluctuating light intensity. *Plant Physiol.* **189**, 375–387 (2022).

29. Wada, S. et al. Flavodiiron protein substitutes for cyclic electron flow without competing CO_2 assimilation in rice. *Plant Physiol.* **176**, 1509–1518 (2018).

30. Kramkowska, M., Grzelak, T. & Czyzewska, K. Benefits and risks associated with genetically modified food products. *Ann. Agric. Environ. Med.* **20**, 413–419 (2013).

31. Kitahata, N. & Asami, T. Chemical biology of abscisic acid. *J. Plant Res.* **124**, 549–557 (2011).

32. Giacomotto, J. & Ségalat, L. High-throughput screening and small animal models, where are we? *Br. J. Pharmacol.* **160**, 204–216 (2010).

33. Lessman, C. A. The developing zebrafish (*Danio rerio*): a vertebrate model for high-throughput screening of chemical libraries. *Birth Defects Res. Part C Embryo Today. Rev.* **93**, 268–280 (2011).

34. Kinoshita, T., Toh, S. & Torii, K. U. Chemical control of stomatal function and development. *Curr. Opin. Plant Biol.* **60**, 102010 (2021).

35. Vaidya, A. S. et al. Dynamic control of plant water use using designed ABA receptor agonists. *Science* **366**, eaaw8848 (2019).

36. Toh, S. et al. Identification and characterization of compounds that affect stomatal movements. *Plant Cell Physiol.* **59**, 1568–1580 (2018).

37. Sakai, Y. et al. The chemical compound bubblin induces stomatal mispatterning in Arabidopsis by disrupting the intrinsic polarity of stomatal lineage cells. *Development* **144**, 499–506 (2017).

38. Bian, C. et al. Protein phosphatase 2A promotes stomatal development by stabilizing SPEECHLESS in Arabidopsis. *Proc. Natl Acad. Sci. USA* **117**, 13127–13137 (2020).

39. Ziadi, A. et al. Discovery of synthetic small molecules that enhance the number of stomata: C–H functionalization chemistry for plant biology. *Chem. Commun.* **53**, 9632–9635 (2017).

40. Kim, J. M. et al. Acetate-mediated novel survival strategy against drought in plants. *Nat. Plants* **3**, 1–7 (2017).

41. Dash, R. R., Gaur, A. & Balomajumder, C. Cyanide in industrial wastewaters and its removal: a review on biotreatment. *J. Hazard. Mater.* **163**, 1–11 (2009).

42. Elsayed, N. M. Toxicity of nitrogen-dioxide—an introduction. *Toxicology* **89**, 161–174 (1994).

43. Yamasaki, T. et al. Temperature acclimation of photosynthesis and related changes in photosystem II electron transport in winter wheat. *Plant Physiol.* **128**, 1087–1097 (2002).

44. Diaz, A. N. Absorption and emission-spectroscopy and photochemistry of 1,10-anthraquinone derivatives—a review. *J. Photochem. Photobiol. A-Chem.* **53**, 141–167 (1990).

45. Uchimiya, M. & Stone, A. T. Reversible redox chemistry of quinones: impact on biogeochemical cycles. *Chemosphere* **77**, 451–458 (2009).

46. Gallmetzer, J. M. et al. Anthraquinone and its derivatives as sustainable materials for electrochemical applications a joint experimental and theoretical investigation of the redox potential in solution. *Phys. Chem. Chem. Phys.* **24**, 16207–16219 (2022).

47. Kim, S. M. et al. Reduction-controlled viologen in bisolvent as an environmentally stable n-type dopant for carbon nanotubes. *J. Am. Chem. Soc.* **131**, 327–331 (2009).

48. Khorobrykh, S., Havurinne, V., Mattila, H. & Tyystjärvi, E. Oxygen and ROS in photosynthesis. *Plants* **9**, 91 (2020).

49. Kato, Y., Sugiura, M., Oda, A. & Watanabe, T. Spectroelectrochemical determination of the redox potential of pheophytin a, the primary electron acceptor in photosystem II. *Proc. Natl Acad. Sci. USA* **106**, 17365–17370 (2009).

50. Sonoike, K. Selective photoinhibition of photosystem I in isolated thylakoid membranes from cucumber and spinach. *Plant Cell Physiol.* **36**, 825–830 (1995).

51. Nishimi T., Kamachi T., Kato K., Kato T., Yoshizawa K. *Mechanistic Study on the Production of Hydrogen Peroxide in the Anthraquinone Process*. (Wiley Online Library, 2011).

52. Wada, K. C. & Takeno, K. Stress-induced flowering. *Plant Signal. Behav.* **5**, 944–947 (2010).

53. Huang, J., Zhao, X. & Chory, J. The Arabidopsis transcriptome responds specifically and dynamically to high light stress. *Cell Rep.* **29**, 4186–4199 (2019).

54. Strotmann, H., Brendel, K., Boos, K. S. & Schlimme, E. Energy transfer inhibition in photosynthesis by anthraquinone dyes. *FEBS Lett.* **145**, 11–15 (1982).

55. Oettmeier, W., Masson, K. & Donner, A. Anthraquinone inhibitors of photosystem-II electron-transport. *FEBS Lett.* **231**, 259–262 (1988).

56. Conrath, U. et al. Priming: getting ready for battle. *Mol. Plant-Microbe Interact.* **19**, 1062–1071 (2006).

57. Martinez-Medina, A. et al. Recognizing plant defense priming. *Trends Plant Sci.* **21**, 818–822 (2016).

58. Kitajima, M. & Butler, W. L. Quenching of chlorophyll fluorescence and primary photochemistry in chloroplasts by dibromothymoquinone. *Biochim. Biophys. Acta* **376**, 105–115 (1975).

59. Nybakken, L., Solhaug, K. A., Bilger, W. & Gauslaa, Y. The lichens *Xanthoria elegans* and *Cetraria islandica* maintain a high protection against UV-B radiation in Arctic habitats. *Oecologia* **140**, 211–216 (2004).

60. Diaz-Munoz, G., Miranda, I. L., Sartori, S. K., de Rezende, D. C. & Diaz, M. A. Anthraquinones: an overview. *Stud. Nat. Products Chem.* **58**, 313–338 (2018).

61. Routoula, E. & Patwardhan, S. V. Degradation of anthraquinone dyes from effluents: a review focusing on enzymatic dye degradation with industrial potential. *Environ. Sci. Technol.* **54**, 647–664 (2020).

62. Wang, J., Li, H., Jin, C., Qu, Y. & Xiao, X. Development and validation of a UPLC method for quality control of rhubarb-based medicine: fast simultaneous determination of five anthraquinone derivatives. *J. Pharm. Biomed. Anal.* **47**, 765–770 (2008).

63. DeLiberto, S. T. & Werner, S. J. Review of anthraquinone applications for pest management and agricultural crop protection. *Pest Manag. Sci.* **72**, 1813–1825 (2016).

64. Brachmann, A. O. et al. A type II polyketide synthase is responsible for anthraquinone biosynthesis in *Photorhabdus luminescens*. *ChemBioChem* **8**, 1721–1728 (2007).

65. Kang, S. H. et al. De novo transcriptome assembly of *Senna occidentalis* sheds light on the anthraquinone biosynthesis pathway. *Front. Plant Sci.* **12**, 773553 (2022).

66. Kang, S. H. et al. Genome-enabled discovery of anthraquinone biosynthesis in *Senna tora*. *Nat. Commun.* **11**, 5875 (2020).

67. Zhou, T. et al. Tissue-specific transcriptome for *Rheum tanguticum* reveals candidate genes related to the anthraquinones biosynthesis. *Physiol. Mol. Biol. Plants* **27**, 2487–2501 (2021).

68. Ruban, A. V. Quantifying the efficiency of photoprotection. *Philos. Trans. R. Soc. B: Biol. Sci.* **372**, 20160393 (2017).

69. Klughammer, C. & Schreiber, U. An improved method, using saturating light pulses, for the determination of photosystem I quantum yield via $P700^+$-absorbance changes at 830 nm. *Planta* **192**, 261–268 (1994).

70. Porra, R. J., Thompson, W. A. & Kriedemann, P. E. Determination of accurate extinction coefficients and simultaneous equations for assaying chlorophylls a and b extracted with four different solvents: verification of the concentration of chlorophyll standards by atomic absorption spectroscopy. *Biochim. Biophys. Acta (BBA)-Bioenerg.* **975**, 384–394 (1989).

71. Terashima, I., Huang, L. K. & Osmond, C. B. Effects of leaf chilling on thylakoid functions, measured at room temperature, in *Cucumis sativus L.* and *Oryza sativa L. Plant Cell Physiol.* **30**, 841–850 (1989).

72. Yamori, W., Noguchi, K., Kashino, Y. & Terashima, I. The role of electron transport in determining the temperature dependence of the photosynthetic rate in spinach leaves grown at contrasting temperatures. *Plant Cell Physiol.* **49**, 583–591 (2008).

73. Kamitani, M., Kashima, M., Tezuka, A. & Nagano, A. J. Lasy-Seq: a high-throughput library preparation method for RNA-Seq and its application in the analysis of plant responses to fluctuating temperatures. *Sci. Rep.* **9**, 7091 (2019).

74. Bolger, A. M., Lohse, M. & Usadel, B. Trimmomatic: a flexible trimmer for Illumina sequence data. *Bioinformatics* **30**, 2114–2120 (2014).

75. Dobin, A. et al. STAR: ultrafast universal RNA-seq aligner. *Bioinformatics* **29**, 15–21 (2013).

76. Li, B. & Dewey, C. N. RSEM: accurate transcript quantification from RNA-Seq data with or without a reference genome. *BMC Bioinforma.* **12**, 323 (2011).

77. Love, M. I., Huber, W. & Anders, S. Moderated estimation of fold change and dispersion for RNA-seq data with DESeq2. *Genome Biol.* **15**, 550 (2014).

78. Wu, T. et al. ClusterProfiler 4.0: a universal enrichment tool for interpreting omics data. *Innovation* **2**, 100141 (2021).

Competing interests
The authors declare no competing interests.

Additional information
Supplementary information The online version contains supplementary material available at https://doi.org/10.1038/s42003-025-07582-2.

Correspondence and requests for materials should be addressed to Wataru Yamori.

Peer review information *Communications Biology* thanks Micaela Carvajal, Nenghui Ye and the other, anonymous, reviewer(s) for their contribution to the peer review of this work. Primary handling editors: Showkat Ganie and David Favero.

Reprints and permissions information is available at http://www.nature.com/reprints

Publisher's note Springer Nature remains neutral with regard to jurisdictional claims in published maps and institutional affiliations.